Local Mesh Refinement

Marc Dröge

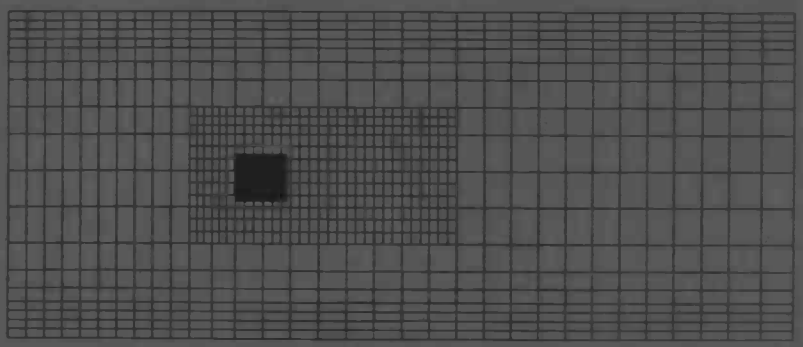

Department of
Mathematics

RuG

Master's thesis

Local Mesh Refinement

Marc Dröge

University of Groningen
Department of Mathematics
P.O. Box 800
9700 AV Groningen

October 2000

Contents

Chapter 1

Introduction

Direct Numerical Simulation of the flow around an object is one of the most challenging applications of Computation Fluid Dynamics. For these simulations a very efficient and robust finite volume discretization method of the Navier-Stokes equations has been developed at the University of Groningen over the years.
In the original version of the method the equations are discretized with a finite volume scheme on a regular grid. This discretization has the disadvantage that refinement in a desired region of the computational domain also alters the grid outside this region, as grid lines are continued to the boundary of the computational domain. Through this inefficient behaviour, regular grids are a major restriction. Local mesh refinement can be the solution to this problem.

In this Master's thesis the development of a general applicable local mesh refinement method is described. First, the discretization of the Navier-Stokes equations on regular grids will be explained. Then local mesh refinement will be introduced and in particular the discretization at the boundary of the refinement. The main property of the discretization is energy conservation. We will examine if it is possible to conserve mass, momentum and energy also at the boundary of the refinement.

Chapter 2

Mathematical Model

The motion of the fluid is governed by conservation laws for mass and momentum. We give these equations in conservation form for a Cartesian co-ordinate system. We will assume that the flow can be considered as incompressible and scale the density ρ to one. Then for every domain Ω with boundary Γ and an outward directed normal vector $\mathbf{n}$ the following equations should hold:

- *conservation of mass* (continuity equation)

$$\int_\Gamma \mathbf{u} \cdot \mathbf{n}\, d\Gamma = 0, \tag{2.1}$$

- *conservation of momentum* (Navier-Stokes equations)

$$\frac{\mathrm{d}}{\mathrm{d}t} \int_\Omega \mathbf{u}\, d\Omega = -\int_\Gamma \mathbf{u}\,(\mathbf{u} \cdot \mathbf{n})\, d\Gamma - \int_\Gamma pI \cdot \mathbf{n}\, d\Gamma + \int_\Gamma \nu \operatorname{grad} \mathbf{u} \cdot \mathbf{n}\, d\Gamma + \int_\Omega \mathbf{F}\, d\Omega, \tag{2.2}$$

where $\mathbf{u} = (u, v, w)^{\mathrm{T}}$ denotes the velocity, t the time, p the pressure, ν the kinematic viscosity and F the external force.
Equations (2.1) and (2.2) will be discretized using the finite volume technique. However, we will mention the conservation laws in differential form, because the different terms will sometimes be referred to in this form.

$$\operatorname{div} \mathbf{u} = 0, \tag{2.3a}$$

$$\frac{\partial \mathbf{u}}{\partial t} + \operatorname{div}(\mathbf{u}\mathbf{u}^{\mathrm{T}}) = -\operatorname{div}(pI) + \operatorname{div}(\nu \operatorname{grad} \mathbf{u}) + \mathbf{F}, \tag{2.3b}$$

Here I is the identity matrix and the divergence of a symmetric matrix is defined as

$$\operatorname{div} \begin{pmatrix} a_1 & a_2 & a_3 \\ a_2 & b_2 & b_3 \\ a_3 & b_3 & c_3 \end{pmatrix} := \begin{pmatrix} \operatorname{div}(a_1\ a_2\ a_3)^{\mathrm{T}} \\ \operatorname{div}(a_2\ b_2\ b_3)^{\mathrm{T}} \\ \operatorname{div}(a_3\ b_3\ c_3)^{\mathrm{T}} \end{pmatrix}.$$

Chapter 3

Numerical Model

3.1 Spatial discretization

The two conservation laws are discretized on a stretched and totally staggered Cartesian grid using a finite volume discretization. Although the discretization is three dimensional, it is explained for the two-dimensional case. See Figure 3.1 for the placement and numbering of the variables.

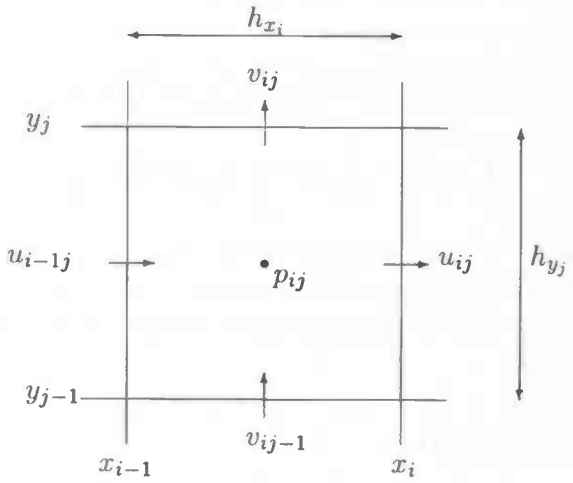

Figure 3.1: Placement of variables in cell (i, j)

3.1.1 Pressure equation

We will start with the discretization of the law of conservation of mass (2.1). For the domain Ω with boundary Γ we will take the cell as drawn in Figure 3.1 and we will call this cell a p-cell. If the eastern, northern, western and southern boundaries are denoted by E, N, W

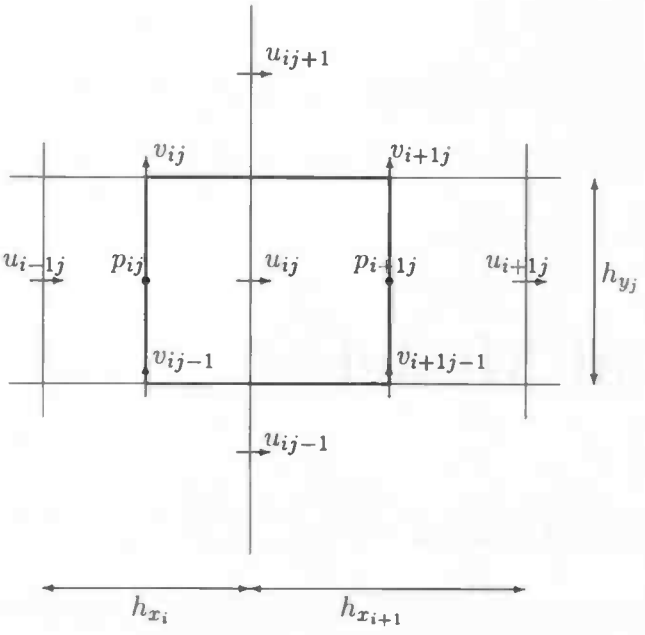

Figure 3.2: Control volume for discretization in x-direction

and S respectively, the pressure equation can be written as

$$\int_E u \, \mathrm{d}y + \int_N v \, \mathrm{d}x - \int_W u \, \mathrm{d}y - \int_S v \, \mathrm{d}x = 0.$$

These four mass fluxes will be denoted as $\bar{u}_{ij}$, $\bar{v}_{ij}$, $\bar{u}_{i-1j}$ and $\bar{v}_{ij-1}$ respectively. We will discretize these integrals with the midpoint rule, so $\bar{u}_{ij} = u_{ij} h_{y_j}$, but for the moment this is not important to know, since the bar notation enables us to use mass fluxes without telling how they are discretized.

3.1.2 Momentum equation

We recall the momentum equation in the x-direction without the external force term,

$$\frac{\mathrm{d}}{\mathrm{d}t} \int_\Omega u \, \mathrm{d}\Omega \;=\; -\int_\Gamma u(\boldsymbol{u} \cdot \boldsymbol{n}) \, \mathrm{d}\Gamma - \int_\Gamma \mathbf{P} \cdot \boldsymbol{n} \, \mathrm{d}\Gamma + \int_\Gamma \nu \, \mathrm{grad}\, u \cdot \boldsymbol{n} \, \mathrm{d}\Gamma, \tag{3.1}$$

with $\mathbf{P} = (p/\rho, 0, 0)^{\mathrm{T}}$ in three space dimensions. For the control volume Ω we will use the boldfaced rectangle (u-cell) in Figure 3.2.
The discretization of the volume integral is given by

$$\int_\Omega u \, \mathrm{d}\Omega \;\doteq\; \Omega_{ij} u_{ij},$$

with $\Omega_{ij} = \frac{h_{x_i} + h_{x_{i+1}}}{2} h_{y_j}$ the volume of the u-cell.

Convection

Now we look at the discretization of

$$\int_\Gamma u(\boldsymbol{u}\cdot\boldsymbol{n})\,\mathrm{d}\Gamma,$$

which is the convective part of Equation (3.1). It is important to understand the meaning of this term: it describes the way the horizontal velocity (in fact horizontal momentum) u is transported by the vector field $\boldsymbol{u}$. This vector field contains u as component as well, but we should treat both u's as different factors.
Again we denote the four boundaries with E, N, W and S and approximate the integrals:

$$\begin{aligned}\int_\Gamma u(\boldsymbol{u}\cdot\boldsymbol{n})\,\mathrm{d}\Gamma &\doteq \frac{u_{ij}+u_{i+1j}}{2}\int_E \boldsymbol{u}\cdot\boldsymbol{n}\,\mathrm{d}y+\frac{u_{ij}+u_{ij+1}}{2}\int_N \boldsymbol{u}\cdot\boldsymbol{n}\,\mathrm{d}x+\\ &\quad \frac{u_{ij}+u_{i-1j}}{2}\int_W \boldsymbol{u}\cdot\boldsymbol{n}\,\mathrm{d}y+\frac{u_{ij}+u_{ij-1}}{2}\int_S \boldsymbol{u}\cdot\boldsymbol{n}\,\mathrm{d}x\\ &= \frac{u_{ij}+u_{i+1j}}{2}\int_E u\,\mathrm{d}y+\frac{u_{ij}+u_{ij+1}}{2}\int_N v\,\mathrm{d}x-\\ &\quad \frac{u_{ij}+u_{i-1j}}{2}\int_W u\,\mathrm{d}y-\frac{u_{ij}+u_{ij-1}}{2}\int_S v\,\mathrm{d}x.\end{aligned}$$

The left integrals are mass fluxes. For the pressure equation we already defined how to compute mass fluxes, but these fluxes are defined at other boundaries. But there is an extra demand that these fluxes have to satisfy: the coefficient of u_{ij} has to be zero. This is necessary if energy is conserved, which will be discussed later. The coefficient of u_{ij} equals

$$\int_E u\,\mathrm{d}y+\int_N v\,\mathrm{d}x-\int_W u\,\mathrm{d}y-\int_S v\,\mathrm{d}x. \tag{3.2}$$

One way to let this equal zero is

$$\begin{aligned}\int_E u\,\mathrm{d}y &= \frac{\bar{u}_{ij}+\bar{u}_{i+1j}}{2},\\ \int_N v\,\mathrm{d}x &= \frac{\bar{v}_{ij}+\bar{v}_{i+1j}}{2},\\ \int_W u\,\mathrm{d}y &= \frac{\bar{u}_{ij}+\bar{u}_{i-1j}}{2},\\ \int_S v\,\mathrm{d}x &= \frac{\bar{v}_{ij-1}+\bar{v}_{i+1j-1}}{2}.\end{aligned}$$

If we substitute this in Equation (3.2) we get

$$\begin{aligned}&\frac{\bar{u}_{ij}+\bar{u}_{i+1j}}{2}+\frac{\bar{v}_{ij}+\bar{v}_{ij+1}}{2}-\frac{\bar{u}_{ij}+\bar{u}_{i-1j}}{2}-\frac{\bar{v}_{ij}+\bar{v}_{ij-1}}{2} =\\ &\frac{\bar{u}_{i+1j}+\bar{v}_{i+1j}-\bar{u}_{ij}-\bar{v}_{i+1j-1}}{2}+\frac{\bar{u}_{ij}+\bar{v}_{ij}-\bar{u}_{i-1j}-\bar{v}_{ij-1}}{2}.\end{aligned} \tag{3.3}$$

In this last expression we recognize half the sum of the divergence of the p-cells (i,j) and $(i+1,j)$ and therefore the expression equals zero.

The discretization finally results in

$$\begin{aligned} &\frac{u_{i+1j}}{2}\frac{\bar{u}_{ij}+\bar{u}_{i+1j}}{2} + \frac{u_{ij+1}}{2}\frac{\bar{v}_{ij}+\bar{v}_{i+1j}}{2} - \\ &\frac{u_{i-1j}}{2}\frac{\bar{u}_{ij}+\bar{u}_{i-1j}}{2} - \frac{u_{ij-1}}{2}\frac{\bar{v}_{ij-1}+\bar{v}_{i+1j-1}}{2}. \end{aligned} \tag{3.4}$$

Diffusion

The diffusion term

$$\int_\Gamma \nu \text{ grad } \boldsymbol{u}\cdot\boldsymbol{n}\, d\Gamma$$

is split into four parts:

$$\int_\Gamma \nu \text{ grad } \boldsymbol{u}\cdot\boldsymbol{n}\, d\Gamma = \int_E \nu\,\frac{\partial u}{\partial x}\,dy + \int_N \nu\,\frac{\partial u}{\partial y}\,dx - \int_W \nu\,\frac{\partial u}{\partial x}\,dy - \int_S \nu\,\frac{\partial u}{\partial y}\,dx.$$

The derivative are approximated by central differences:

$$\int_E \nu\,\frac{u_{i+1j}-u_{ij}}{h_{x_{i+1}}}\,dy + \int_N \nu\,\frac{u_{ij+1}-u_{ij}}{(h_{y_j}+h_{y_{j+1}})/2}\,dx - \int_W \nu\,\frac{u_{ij}-u_{i-1j}}{h_{x_i}}\,dy - \int_S \nu\,\frac{u_{ij}-u_{ij-1}}{(h_{y_j}+h_{y_{j-1}})/2}\,dx.$$

Next, the integrals are approximated by the midpoint rule:

$$\begin{aligned} &\nu\, h_{y_j}\frac{u_{i+1j}-u_{ij}}{h_{x_{i+1}}} + \nu\,\frac{h_{x_i}+h_{x_{i+1}}}{2}\frac{u_{ij+1}-u_{ij}}{(h_{y_j}+h_{y_{j+1}})/2} - \\ &\nu\, h_{y_j}\frac{u_{ij}-u_{i-1j}}{h_{x_i}} - \nu\,\frac{h_{x_i}+h_{x_{i+1}}}{2}\frac{u_{ij}-u_{ij-1}}{(h_{y_j}+h_{y_{j-1}})/2}. \end{aligned} \tag{3.5}$$

Pressure gradient

The last term in the Navier-Stokes equation is the integral over the pressure. This is also a boundary integral, so

$$\int_\Gamma \mathbf{P}\cdot\boldsymbol{n}\, d\Gamma \doteq h_{y_j}p_{i+1j} + \frac{h_{x_i}+h_{x_{i+1}}}{2}\,0 - h_{y_j}p_{ij} + \frac{h_{x_i}+h_{x_{i+1}}}{2}\,0 = h_{y_j}p_{i+1j} - h_{y_j}p_{ij}.$$

Upwind

The discretization of the convective term was a central discretization. For upwind discretization we introduce an upwind parameter α. We take α between 0 and 1. When α equals zero the discretization is central and when α equals one an upwind discretization is used. The upwind discretization comes in as artificial diffusion, so we have to replace all ν's by $\nu+\nu_a$. We will only discuss the change of the first term. The coefficient of u_{i+1j}, consisting of a convective and a diffusive part, is replaced by

$$-\left(\frac{\bar{u}_{ij}+\bar{u}_{i+1j}}{4} - h_{y_j}\frac{\nu+\alpha\nu_{a_e}}{h_{x_i}}\right),$$

with $\nu_{a_e} = \frac{1}{4}|u_{i+1j}+u_{ij}|h_{x_{i+1}}$.

Remarks

Some approximations in the discretization may look somewhat arbitrary, but this is certainly not the case. If Expression (3.4) is written in matrix notation, like

$$C(\bar{u}, \bar{v})u,$$

it is easily seen that the coefficient matrix C is skew-symmetric. Furthermore, after rearranging (3.5) to

$$\begin{aligned} &\nu \frac{h_{y_j}}{h_{x_{i+1}}} u_{i+1j} + \nu \frac{h_{x_i}+h_{x_{i+1}}}{h_{y_j}+h_{y_{j+1}}} u_{ij+1} + \\ &\nu \frac{h_{y_j}}{h_{x_i}} u_{i-1j} + \nu \frac{h_{x_i}+h_{x_{i+1}}}{h_{y_j}+h_{y_{j-1}}} u_{ij-1} - \\ &\nu \left(\frac{h_{y_j}}{h_{x_{i+1}}} + \frac{h_{x_i}+h_{x_{i+1}}}{h_{y_j}+h_{y_{j+1}}} + \frac{h_{y_j}}{h_{x_i}} + \frac{h_{x_i}+h_{x_{i+1}}}{h_{y_j}+h_{y_{j-1}}}\right) u_{ij} \end{aligned}$$

it may be noticed that the diffusion matrix (with a minus sign) is symmetric and weakly diagonally dominant. This implies that its eigenvalues are all real and positive. Later we will see that these properties of the convection and diffusion are necessary for energy conservation. The discretization in the y- and z-direction is done in the same manner. The discretization is easily extended to three dimensions.

3.2 Time discretization

We will now consider the time discretization of the system

$$\int_\Gamma \boldsymbol{u} \cdot \boldsymbol{n} \, \mathrm{d}\Gamma = 0, \tag{3.6}$$

$$\frac{\mathrm{d}}{\mathrm{d}t} \int_\Omega \boldsymbol{u} \, \mathrm{d}\Omega = \int_\Gamma -\boldsymbol{u}(\boldsymbol{u} \cdot \boldsymbol{n}) \, \mathrm{d}\Gamma + \int_\Gamma \nu \, \mathrm{grad}\, \boldsymbol{u} \cdot \boldsymbol{n} \, \mathrm{d}\Gamma - \int_\Gamma p\boldsymbol{I} \cdot \boldsymbol{n} \, \mathrm{d}\Gamma. \tag{3.7}$$

If $\mathbf{R}(u)$ is substituted for the convective and diffusive terms, Equation (3.7) can be written as

$$\frac{\mathrm{d}}{\mathrm{d}t} \int_\Omega \boldsymbol{u} \, \mathrm{d}\Omega = \mathbf{R}(u) - \int_\Gamma p\boldsymbol{I} \cdot \boldsymbol{n} \, \mathrm{d}\Gamma.$$

After applying the divergence operator we find

$$\frac{\mathrm{d}}{\mathrm{d}t} \int_\Gamma \boldsymbol{u} \cdot \boldsymbol{n} \, \mathrm{d}\Gamma = \mathrm{div}(\mathbf{R}(u)) - \mathrm{div} \int_\Gamma p\boldsymbol{I} \cdot \boldsymbol{n} \, \mathrm{d}\Gamma.$$

The left hand side equals zero (Equation (3.6)) and the last term is a Laplace operator ($\mathrm{div} \cdot \mathrm{div}^T$). If an explicit time integration method is used, $\mathbf{R}$ is evaluated at a new time step, so the $\mathrm{div}(\mathbf{R}(u))$ term can be evaluated in advance. The resulting equation is a Poisson equation for the pressure.
We can follow the same recipe for the spatial discretized equations. The divergence operator is the one defined on p-cells, the $\int_\Gamma p\boldsymbol{I} \cdot \boldsymbol{n} \, \mathrm{d}\Gamma$ operator is defined on u-, v- and w-cells. Analytically, these operators are adjoins (div and $-$grad respectively) and we will show that this property also holds after discretization. This result will be used later to prove energy conservation. We will take a small grid and construct the divergence operator (see Figure 3.3).

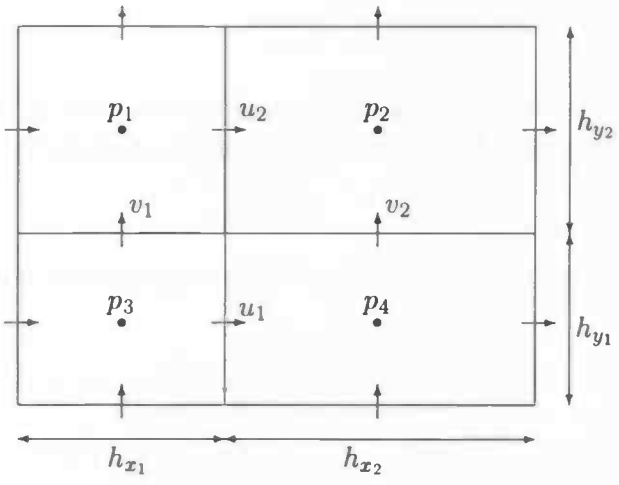

Figure 3.3: Grid consisting of four cells

The divergence of u is given by

$$\begin{bmatrix} & h_{y_2} & -h_{x_1} & \\ & -h_{y_2} & & -h_{x_2} \\ h_{y_1} & & h_{x_1} & \\ -h_{y_1} & & & h_{x_2} \end{bmatrix} \begin{bmatrix} u_1 \\ u_2 \\ v_1 \\ v_2 \end{bmatrix}.$$

Then

$$-\mathrm{div}^{\mathrm{T}} p = \begin{bmatrix} & & -h_{y_1} & h_{y_1} \\ -h_{y_2} & h_{y_2} & & \\ h_{x_1} & & -h_{x_1} & \\ & h_{x_2} & & -h_{x_1} \end{bmatrix} \begin{bmatrix} p_1 \\ p_2 \\ p_3 \\ p_4 \end{bmatrix}$$

and this is exactly the way the pressure gradient was defined in the previous section. So the "div=-grad" property also holds in the discretized case.

3.3 Energy conservation

There seems to be some freedom in defining the momentum fluxes, but there is an additional equation we should satisfy. Therefore we will introduce the energy of the flow, which is the integral of $\frac{1}{2}\rho|u|^2$. After discretization we will denote this as the inner product $\frac{1}{2}(\!(\Omega u, u)\!)$, where the density is omitted and Ω contains the local grid size. If we denote the convective term with $C(\bar{u})u$, the diffusive term as Du and the pressure term as Mp, then the spatial discretized Navier-Stokes equations and continuity equation can be written as

$$\frac{\mathrm{d}}{\mathrm{d}t}\Omega u = Cu - Du + Mp, \qquad M^* u = 0.$$

We can now write the equation for the change of energy as

$$\begin{aligned} \frac{\mathrm{d}}{\mathrm{d}t}(\!(\Omega u, u)\!) &= (\!(\frac{\mathrm{d}}{\mathrm{d}t}\Omega u, u)\!) + (\!(\Omega u, \frac{\mathrm{d}}{\mathrm{d}t} u)\!) \\ &= (\!(Cu, u)\!) - (\!(Du, u)\!) + (\!(Mp, u)\!) + (\!(u, Cu)\!) - (\!(u, Du)\!) + (\!(u, Mp)\!) \\ &= (\!((C + C^*)u, u)\!) - (\!((D + D^*)u, u)\!) + (\!(p, M^* u)\!) + (\!(M^* up)\!). \end{aligned}$$

Since we have discretized in such a way that the matrix C is skew-symmetric, the convective term is zero. The diffusive term is negative, since the symmetric matrix D is positive definite. Analytically, both pressure terms are zero, since M is the $-$gradient operator and therefore M^* is the divergence. The divergence of the velocity is zero because of mass conservation. Since the discrete gradient operator is chosen such that it is minus the divergence operator, this property also holds after discretization in our case.
So the discretized system has the same properties as the analytical system: convection and pressure do not change the kinetic energy and diffusion is always dissipative. Besides this, the kinetic energy in simulations can also never increase. This is a big advantage, since it implies that the simulation cannot 'explode'; the velocity field may have some wiggles if the grid is too coarse, but these wiggles can never grow large.
The required condition for energy conservation for the convection is a skew-symmetric matrix. This is easily achieved by taking the weights $\frac{1}{2}$ for the mean velocity at the cell boundary. Besides, the central coefficient (the diagonal of the matrix) has to be zero. This means that both p-cells wherein the u-, v- or w-cell is contained have to be divergence free.
The pressure conserves energy if the gradient equals minus the transpose of the divergence. These divergence and gradient operators should of course be consistently used in the momentum equations.

Chapter 4

Local Mesh Refinement

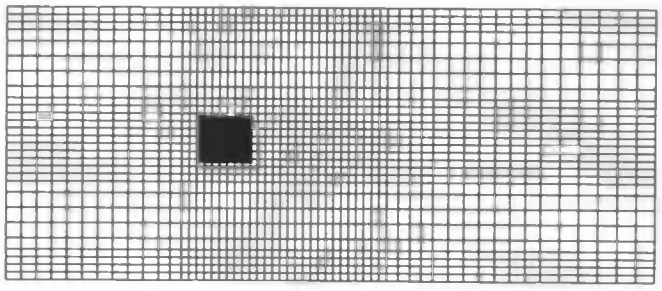

Figure 4.1: Grid without local refinement (1653 cells).

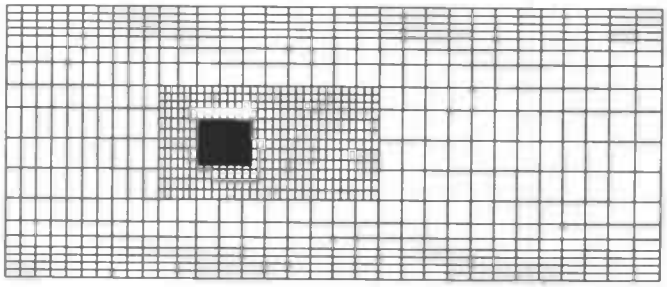

Figure 4.2: Grid with local refinement (947 cells).

The purpose of local mesh refinement is to refine only parts of the computational domain where more accuracy is needed. An example of this is a channel flow around a cube. If, in this case, is refined around the cube, a whole '+'-shaped area is refined, as is illustrated in Figure 4.1. With local mesh refinement, on the contrary, only within a rectangle is refined (Figure 4.2). Huge amounts of grid cells can be saved with local mesh refinement.
One problem that occurs with local mesh refinement is the storage of the new variables. There are a few solutions to this problem, all with advantages and disadvantages. We will discuss two ways of storage.

- All new variables are stored together in a new array. The refined cells are numbered

and this number is an index for the array with the refined variables. This method has a few advantages. It is flexible: it is no problem if more than one area is refined and multiple levels of refinement are possible. The major disadvantage of this method is its inefficiency. The refined variables will be addressed indirectly and if-statements within loops, to determine whether a cell and its neighbours are refined, are unavoidable.

- If the area that is refined is limited to a rectangle, it is possible to use a new 'regular' array, which has the same indices as the normal cells. The biggest disadvantage of this method is its inflexibility; only one rectangular area can be refined. But this approach is very efficient. Indirect addressing could easily cause problems on supercomputers and this is avoided now.

The choice seems to be between efficiency on the one side and flexibility on the other. Since the main purpose of the local mesh refinement is simulating turbulent flow around objects, one rectangular refined area is not a limitation. Furthermore, it is important that the program runs efficiently on supercomputers. Therefore, the second variant is chosen.
In general it is possible to refine only in one direction or in two or three. This is not easy to catch in a general formulation, and refinement is always done in two directions. The third direction is Fourier transformed for the flow around objects and can therefore not be refined. In Figure 4.3 the names and numbering of the new variables is defined.

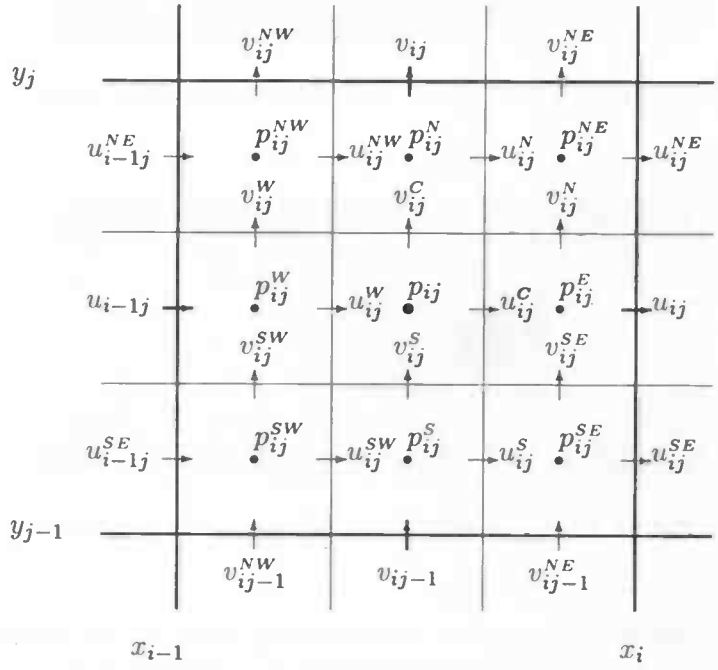

Figure 4.3: Names of variables in a refined cell.

The discretization within the refined area is no problem, since the mesh is just as 'normal'. The same holds for the area outside the refinement. The difficulty is the boundary of the refinement. We will only describe the discretization at the right/eastern boundary of the refinement. The discretization at the other boundaries is obtained by means of mirroring or

rotating. Furthermore, in the examples we will only refine in one direction, which is analogous to strong stretching if only refinement at one boundary is considered. With this the problem is reduced to writing down the discretization of the grid in Figure 4.4. The encircled velocity vectors are missing one or two neighbours. More specifically, the encircled vertical velocities are missing an eastern neighbour for defining a mean velocity at the eastern boundary of a v-cell. The horizontal velocities are missing one northern/southern vertical velocity for the mass flux through the northern/southern u-cell and furthermore an eastern horizontal velocity for the mean velocity and mass flux at the eastern boundary of the u-cell. How we will solve this will be discussed in detail later. In the next chapter we will first focus on the pressure equation.

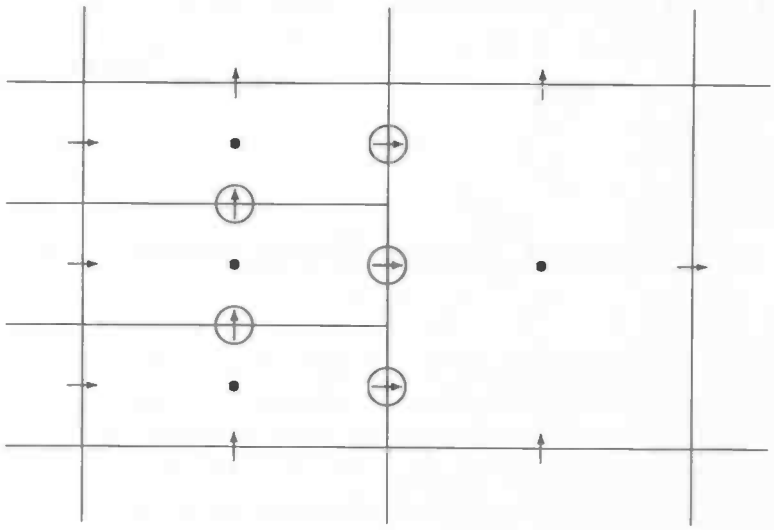

Figure 4.4: Boundary of refinement (vectors are velocities, pressure is defined at dots).

Chapter 5

Discretization at Boundary of Refinement

5.1 Mass conservation at refinement boundary

Looking at Figure 4.4 one may notice that two of the three pressures of the small cells are missing an eastern neighbour. This problem is easily avoided if the pressure in the big cell is assumed constant in its whole p-cell. Then all three 'small' pressures share the same eastern neighbour. We will work this idea out for a simple test case. We will choose boundary conditions for a uniform flow in the y-direction, see Figure 5.1.

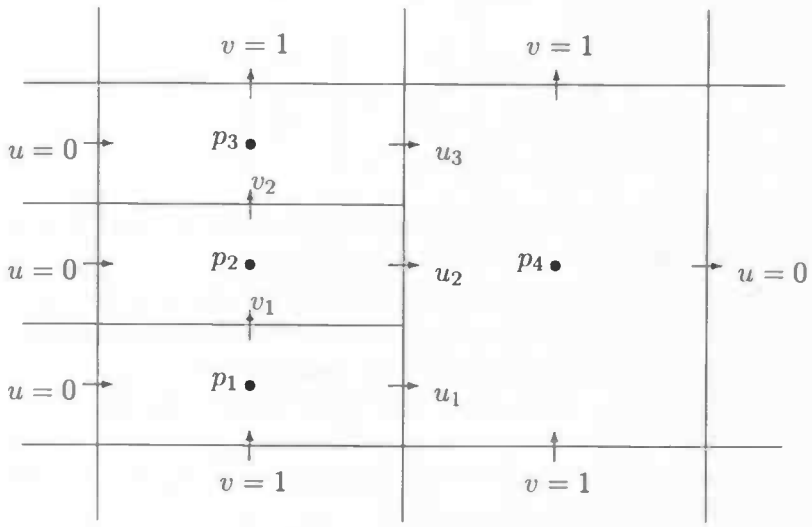

Figure 5.1: Simple test case for pressure.

The discrete Laplace operator is constructed as $\mathrm{div} \cdot \Omega^{-1} \cdot \mathrm{div}^T$ with omega the diagonal matrix containing the u- and v-cell sizes. If the width and height of the unrefined cell both equal

one, then

$$\text{div } u = \begin{bmatrix} \frac{1}{3} & & & 1 & \\ & \frac{1}{3} & & -1 & 1 \\ & & \frac{1}{3} & & -1 \\ -\frac{1}{3} & -\frac{1}{3} & -\frac{1}{3} & & \end{bmatrix} \begin{bmatrix} u_1 \\ u_2 \\ u_3 \\ v_1 \\ v_2 \end{bmatrix}$$

and div Ω^{-1} div$^{\mathrm{T}}$ =

$$\begin{bmatrix} \frac{1}{3} & & & 1 & \\ & \frac{1}{3} & & -1 & 1 \\ & & \frac{1}{3} & & -1 \\ -\frac{1}{3} & -\frac{1}{3} & -\frac{1}{3} & & \end{bmatrix} \begin{bmatrix} 3 & & & & \\ & 3 & & & \\ & & 3 & & \\ & & & 3 & \\ & & & & 3 \end{bmatrix} \begin{bmatrix} \frac{1}{3} & & & -\frac{1}{3} \\ & \frac{1}{3} & & -\frac{1}{3} \\ & & \frac{1}{3} & -\frac{1}{3} \\ 1 & -1 & & \\ & 1 & -1 & \end{bmatrix} =$$

$$\begin{bmatrix} \frac{10}{3} & -3 & & -\frac{1}{3} \\ -3 & \frac{19}{3} & -3 & -\frac{1}{3} \\ & -3 & \frac{10}{3} & -\frac{1}{3} \\ -\frac{1}{3} & -\frac{1}{3} & -\frac{1}{3} & 1 \end{bmatrix}. \tag{5.1}$$

The resulting matrix is weakly diagonally dominant and symmetric, so positive-definite as it should be (of course it is singular, **1** is an eigenvector). The right hand side of the Poisson equation, containing the boundary conditions, equals $[\ -1 \quad 0 \quad 1 \quad 0\ ]^{\mathrm{T}}$. Now the solution of the equation div Ω^{-1} div$^{\mathrm{T}}p = [\ -1 \quad 0 \quad 1 \quad 0\ ]^{\mathrm{T}}$ can be computed and yields

$$\begin{bmatrix} p_1 \\ p_2 \\ p_3 \\ p_4 \end{bmatrix} = \begin{bmatrix} \frac{3}{10} \\ 0 \\ -\frac{3}{10} \\ 0 \end{bmatrix}, \qquad \begin{bmatrix} u_1 \\ u_2 \\ u_3 \\ u_4 \end{bmatrix} = \begin{bmatrix} -\frac{3}{10} \\ 0 \\ \frac{3}{10} \\ 0 \end{bmatrix}, \qquad \begin{bmatrix} v_1 \\ v_2 \end{bmatrix} = \begin{bmatrix} \frac{9}{10} \\ \frac{9}{10} \end{bmatrix},$$

where u is computed by $-\Omega^{-1}$ div$^{\mathrm{T}}p$. We may notice two things: each p-cell is divergence free and, more noticeable, 10% of the fluid particles detour.
This defect can be explained as follows. The analytic solution is a pressure field that is linear in the vertical direction. Our solution is linear, but with a wrong coefficient. If we look at the $-$div$^{\mathrm{T}}$ matrix, we notice that the three pressure gradients at u_1, u_2 and u_3 are different if the pressures p_1, p_2 and p_3 differ, which is the case with linear p. So the three pressure gradients will differ and if they differ, they cannot all equal zero as it should be in this example. Instead, two vortices are formed that are invisible for the unrefined cell, but they strongly disturb the flow through the refined cells (see Figure 5.2).
This problem can easily be solved by averaging the three pressure gradients at u_1, u_2 and u_3:

$$\text{div } u = \begin{bmatrix} \frac{1}{9} & \frac{1}{9} & \frac{1}{9} & 1 & \\ \frac{1}{9} & \frac{1}{9} & \frac{1}{9} & -1 & 1 \\ \frac{1}{9} & \frac{1}{9} & \frac{1}{9} & & -1 \\ -\frac{1}{3} & -\frac{1}{3} & -\frac{1}{3} & & \end{bmatrix} \begin{bmatrix} u_1 \\ u_2 \\ u_3 \\ v_1 \\ v_2 \end{bmatrix}.$$

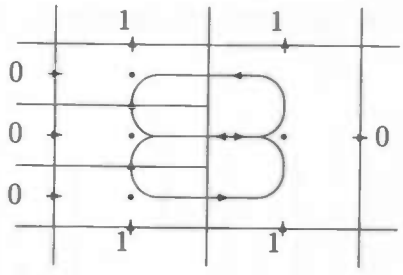

Figure 5.2: Two vortices are formed at the refinement boundary.

With this divergence matrix u_1, u_2 and u_3 have to be equal afterwards and therefore must all be zero. One disadvantage of this method is that its fill deviates from the standard five-points scheme that is common to discrete Laplace operators, since

$$\text{div } \Omega^{-1} \text{ div}^{\mathrm{T}} = \begin{bmatrix} \frac{28}{9} & -\frac{26}{9} & \frac{1}{9} & -\frac{1}{3} \\ -\frac{26}{9} & \frac{55}{9} & -\frac{26}{9} & -\frac{1}{3} \\ \frac{1}{9} & -\frac{26}{9} & \frac{28}{9} & -\frac{1}{3} \\ -\frac{1}{3} & -\frac{1}{3} & -\frac{1}{3} & 1 \end{bmatrix}. \tag{5.2}$$

Furthermore, the diagonally dominance of the matrix is disturbed; in the 3x3 upper left block 1/9 is added with respect to Equation (5.1).
But there is an even bigger problem. By averaging the mass flux we introduced a new defect. This will again be shown by an example. This time we take u linear (in y-direction) and v zero, see Figure 5.3.

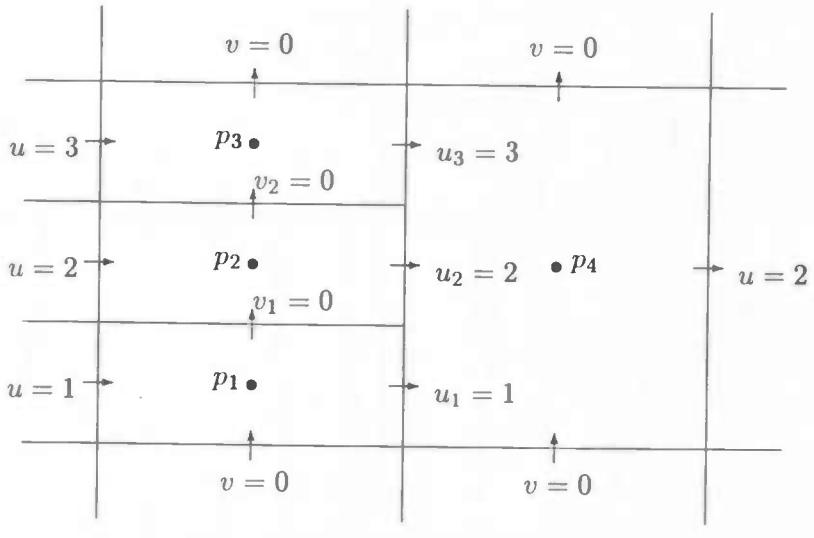

Figure 5.3: Second test case for pressure.

Now we started with a divergence free vector field. Of course, p = constant should be a

solution of the Poisson equation. However, the divergence yields

$$\begin{bmatrix} -\frac{1}{3} \\ -\frac{2}{3} \\ -1 \\ 2 \end{bmatrix} + \begin{bmatrix} \frac{1}{9} & \frac{1}{9} & \frac{1}{9} & 1 & \\ \frac{1}{9} & \frac{1}{9} & \frac{1}{9} & -1 & 1 \\ \frac{1}{9} & \frac{1}{9} & \frac{1}{9} & & -1 \\ -\frac{1}{3} & -\frac{1}{3} & -\frac{1}{3} & & \end{bmatrix} \begin{bmatrix} 1 \\ 2 \\ 3 \\ 0 \\ 0 \end{bmatrix} = \begin{bmatrix} \frac{1}{3} \\ 0 \\ -\frac{1}{3} \\ 0 \end{bmatrix}, \tag{5.3}$$

where the first part originates from the boundary conditions and the second part is div u. So Equation (2.1) is not satisfied in this case and thus the situation of Figure 5.3 cannot occur. The Poisson equation changes the values of v_1 and v_2 to $-1/3$. This may not seem that bad in this example, but at bigger grids it will spoil other velocities as well (p_1, p_2 and p_3 differ and this will also influence the other neighbours).

We will propose a divergence operator that does not have the disadvantages of the former operators. For this divergence operator we will use a larger grid, because the relations will be clearer then. Unfortunately, the matrices will be much larger too and therefore the derivation may look more more difficult than it is. In Figure 5.4 the new grid is drawn.

The column of cells in the middle of the grid is not refined, but cut into three pieces. Instead of one pressure, these cells get three. As usual we start defining div $u =$

$$\begin{bmatrix} \frac{1}{3} & & & & & & & & 1 & & & & & & \\ & \frac{1}{3} & & & & & & & -1 & 1 & & & & & \\ & & \frac{1}{3} & & & & & & & -1 & 1 & & & & \\ & & & \frac{1}{3} & & & & & & & -1 & 1 & & & \\ & & & & \frac{1}{3} & & & & & & & -1 & 1 & & \\ & & & & & \frac{1}{3} & & & & & & & -1 & & \\ & & & & & & \frac{1}{3} & & & & & & & \frac{1}{3} & \\ -\frac{1}{3} & & & & & & \frac{1}{3} & & & & & & & \frac{1}{3} & \\ & -\frac{1}{3} & & & & & \frac{1}{3} & & & & & & & \frac{1}{3} & \\ & & -\frac{1}{3} & & & & \frac{1}{3} & & & & & & & -\frac{1}{3} & \\ & & & -\frac{1}{3} & & & & \frac{1}{3} & & & & & & -\frac{1}{3} & \\ & & & & -\frac{1}{3} & & & \frac{1}{3} & & & & & & -\frac{1}{3} & \\ & & & & & -\frac{1}{3} & & \frac{1}{3} & & & & & & & 1 \\ & & & & & & -1 & & & & & & & & -1 \end{bmatrix} \begin{bmatrix} u_1 \\ u_2 \\ u_3 \\ u_4 \\ u_5 \\ u_6 \\ u_7 \\ u_8 \\ v_1 \\ v_2 \\ v_3 \\ v_4 \\ v_5 \\ v_6 \\ v_7 \end{bmatrix}.$$

Again, Ω is the diagonal matrix containing the sizes of the u- and v-cells, which yields $[\frac{1}{3} \ \frac{1}{3} \ \frac{1}{3} \ \frac{1}{3} \ \frac{1}{3} \ \frac{1}{3} \ 1 \ 1 \ \frac{1}{3} \ \frac{1}{3} \ \frac{1}{3} \ \frac{1}{3} \ \frac{1}{3} \ 1 \ 1]$. Now we can compute the discrete Laplace

operator, yielding

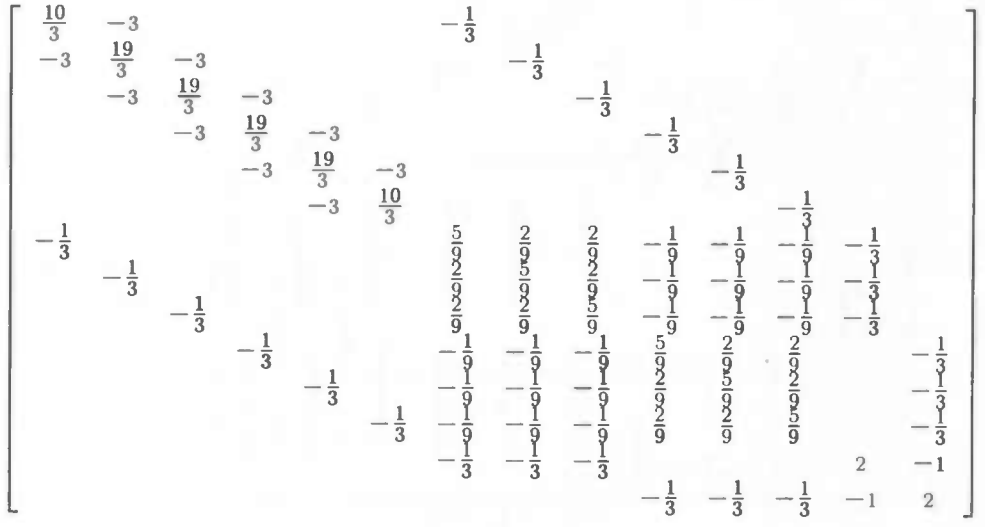

Next, we will define two new pressures, $\tilde{p}_8 = \frac{1}{3}(p_7 + p_8 + p_9)$ and $\tilde{p}_{11} = \frac{1}{3}(p_{10} + p_{11} + p_{12})$, so the mean pressures of the two coarse cells that were cut into three pieces. These definitions are added in the third and fourth row from below of the matrix. At the same time, the sums of the equations for p_7, p_8, p_9 and p_{10}, p_{11}, p_{12} are added:

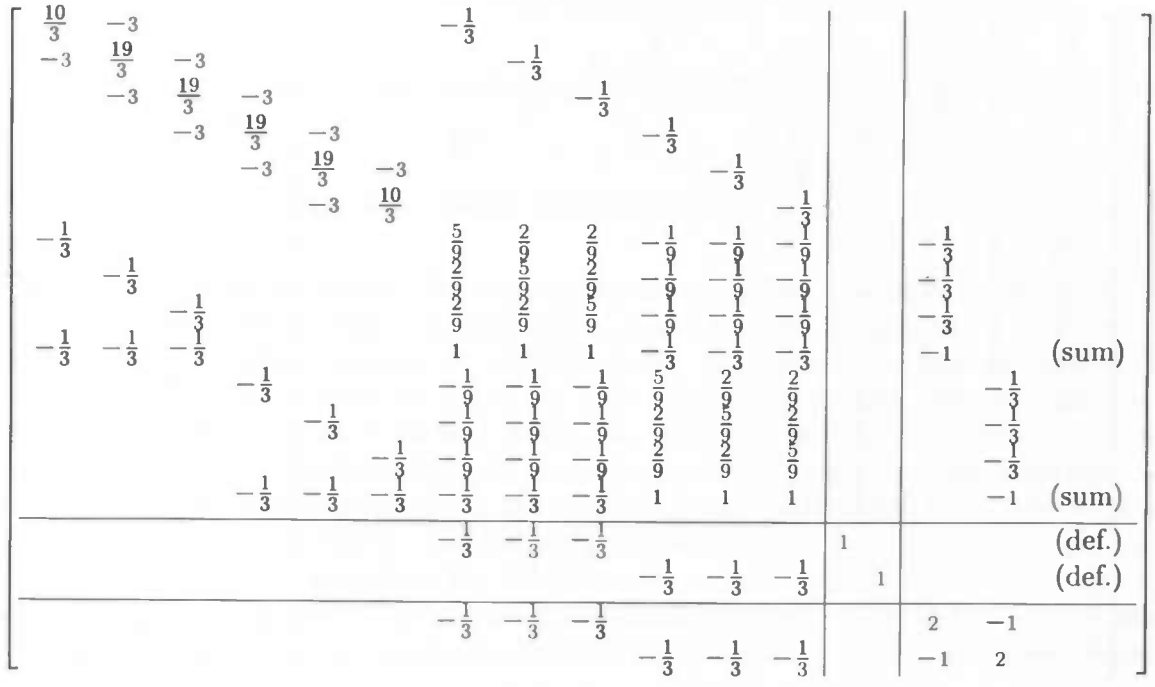

Now $\tilde{p}_8$ and $\tilde{p}_{11}$ are used to sweep the equations for p_{13}, p_{14} and the two new 'sum-equations':

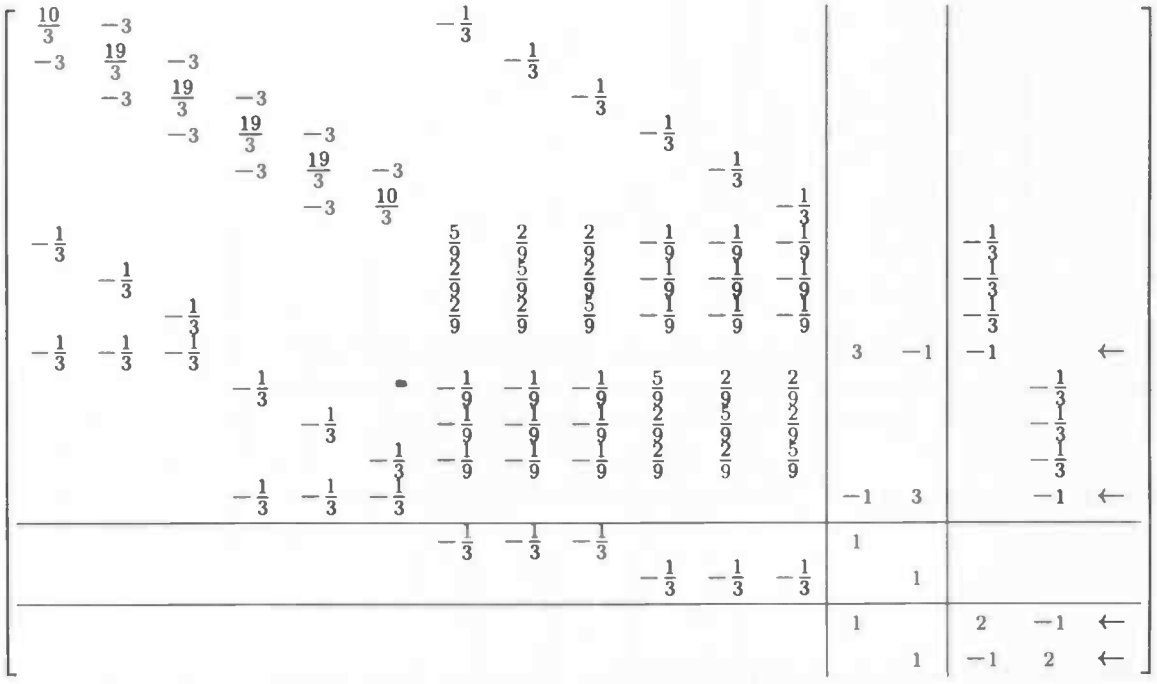

The equations for p_7, p_8, p_9, p_{10}, p_{11} and p_{12} are now swept with $\tilde{p}_8$, $\tilde{p}_{11}$ and the sum-equations. The equations are multiplied by 3 afterwards:

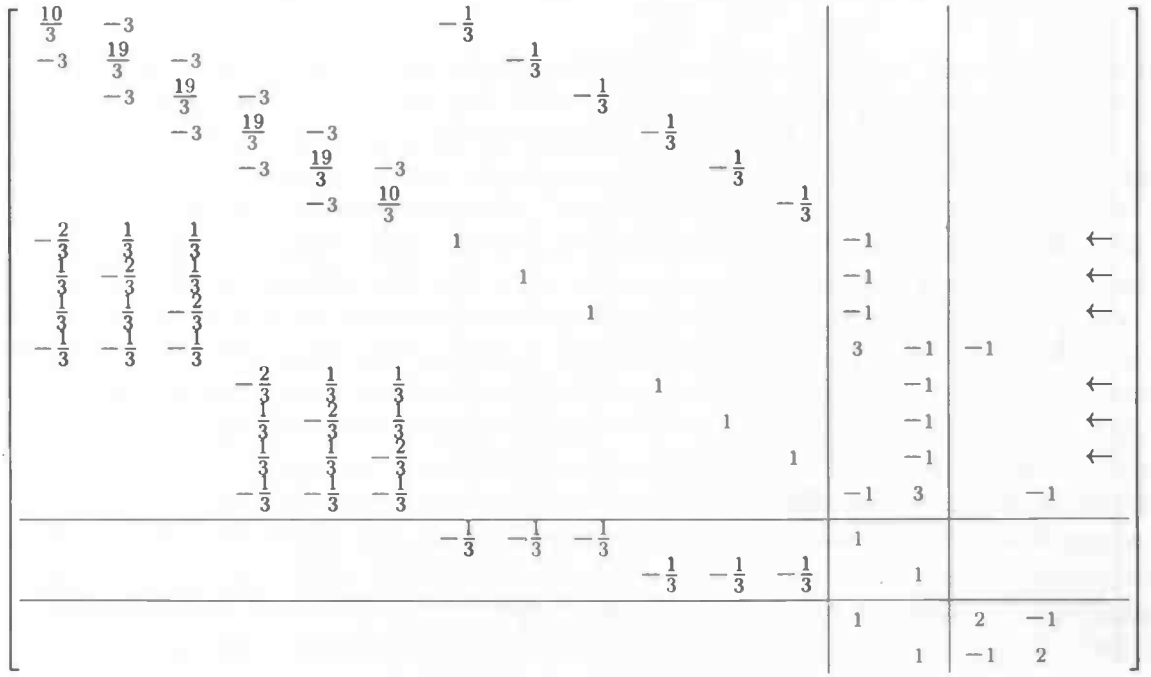

Finally, we throw away the definitions of $\tilde{p}_8$ and $\tilde{p}_{11}$ and rearrange the equations:

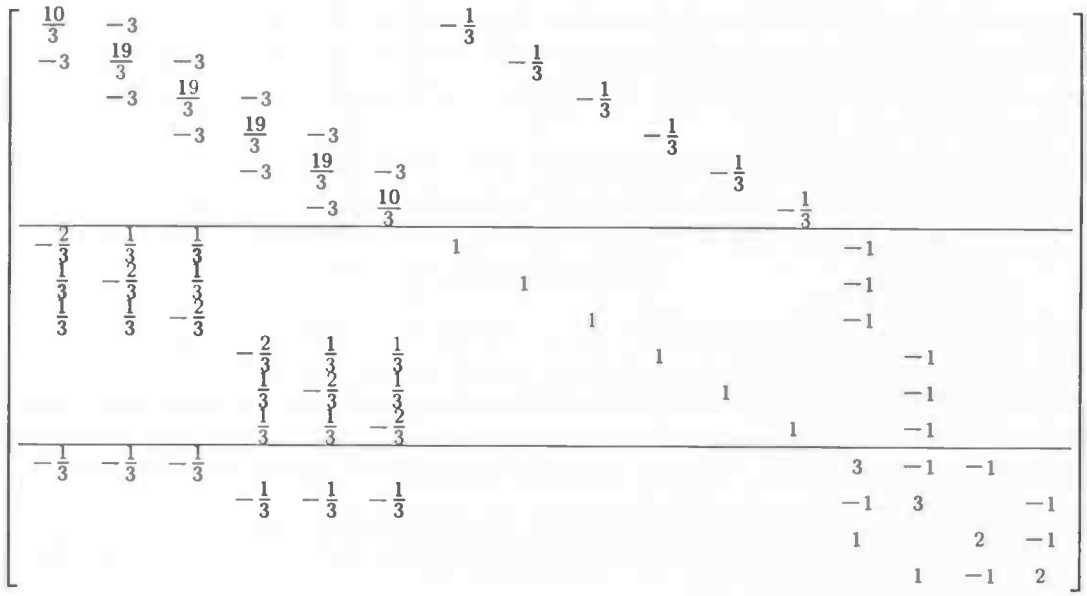

The last four equations are just 'normal' equations, as we had before. The third and fourth equation from below, that were formed as the sum of others, have become equations for $\tilde{p}_8$ and $\tilde{p}_{11}$. The equations for $p_1, \ldots, p_6$ are normal too, but they all have an 'own' eastern neighbour, instead of two shared neighbours (one could say that $p_1, \ldots, p_6$ do not know that their eastern neighbour is not refined). The other six equations in the middle form a connection between $p_7, \ldots, p_{12}$ and $\tilde{p}_8$, $\tilde{p}_{11}$. We will later see that this form eases the implementation of the Poisson solver as well. However, a few questions have still to be answered.

- What is the general form of the coupling equations?
- What happens to the right hand side of the Poisson equation after performing these row operations?
- Does this system handle the former examples well?

The first question is the easiest. The coefficients of the coupling equations are dimensionless and therefore always the same. To answer the second question we will follow the previous procedure again and now focus on the right hand side. We start adding two definitions. The right hand side of these equations are zero. The equations of the sum that are added next have the same right hand side as they would have got if we had treated the cells as being normal. Adding the definitions of $\tilde{p}_8$ and $\tilde{p}_{11}$ has no consequence for the right hand side. We only have to look at the equations for $p_1, \ldots, p_6$. Let us call the right hand sides of these equations $r_1, \ldots, r_6$ respectively. Furthermore, define $\tilde{r}_8$ and $\tilde{r}_{11}$ as the 'normal' right hand sides of the whole cells. Of course, the relations $r_7 + r_8 + r_9 = \tilde{r}_8$ and $r_{10} + r_{11} + r_{12} = \tilde{r}_{11}$ should hold for consistency, which makes the equations for $\tilde{p}_8$ and $\tilde{p}_{11}$ regular. The right hand sides of the equations for $\tilde{p}_8$ and $\tilde{p}_{11}$ we eventually get, are $3r_7 - \tilde{r}_8$ etc. To answer the last

question we will first eliminate the coupling equations from the system, resulting in

$$\begin{bmatrix}
3 & -3 & & & & & \frac{2}{3} & -\frac{1}{3} & -\frac{1}{3} & \\
-3 & 6 & -3 & & & & \frac{2}{3} & -\frac{1}{3} & -\frac{1}{3} & \\
 & -3 & 6 & -3 & & & \frac{2}{3} & -\frac{1}{3} & -\frac{1}{3} & \\
 & & -3 & 6 & -3 & & -\frac{1}{3} & \frac{2}{3} & & -\frac{1}{3} \\
 & & & -3 & 6 & -3 & -\frac{1}{3} & \frac{2}{3} & & -\frac{1}{3} \\
 & & & & -3 & 3 & -\frac{1}{3} & \frac{2}{3} & & -\frac{1}{3} \\
-\frac{1}{3} & -\frac{1}{3} & -\frac{1}{3} & & & & 3 & -1 & -1 & \\
 & & & -\frac{1}{3} & -\frac{1}{3} & -\frac{1}{3} & -1 & 3 & & -1 \\
 & & & & & & -1 & & 2 & -1 \\
 & & & & & & & -1 & -1 & 2
\end{bmatrix}.$$

With this operation the right hand sides of the refined cells have changed. For example, the right hand side of the equation for p_1 equals $r_1 + r_7 - \frac{1}{3}\tilde{r}_8$. For the example of Figure 5.3 this should be zero. In this case r_1 and $\tilde{r}_8$ are both zero, so r_7 should be zero. Therefore is seems logical to define $r_7 = r_8 = r_9 = \frac{1}{3}\tilde{r}_8$ and $r_{10} = r_{11} = r_{12} = \frac{1}{3}\tilde{r}_{11}$.
For simplicity the grid is now reduced to the one of Figure 5.1. The accompanying discrete Poisson matrix simplifies to

$$\begin{bmatrix}
\frac{28}{9} & -\frac{26}{9} & \frac{1}{9} & -\frac{1}{3} \\
-\frac{26}{9} & \frac{55}{9} & -\frac{26}{9} & -\frac{1}{3} \\
\frac{1}{9} & -\frac{26}{9} & \frac{28}{9} & -\frac{1}{3} \\
-\frac{1}{3} & -\frac{1}{3} & -\frac{1}{3} & 1
\end{bmatrix}.$$

This is the same matrix as in Equation (5.2). The right hand side has to be computed differently compared to Equation (5.3). The first test case with uniform velocity is now also no problem, since the matrix is the same as Equation (5.2).

5.2 Poisson solver

The local refinement will lessen the efficiency of the used Poisson solver. On a grid without refinement it is possible to reach all grid nodes with one (nested) loop, but with mesh refinement this is not that easy. One could cut the grid in five pieces or use if-statements within the loop. The first approach makes the source code less surveyable and the second is not efficient, especially not on supercomputers. It is very important that the Poisson solver is efficient, since most simulation time consists of the pressure solve. To avoid these difficulties a multilevel method is used. We will show that, when using this technique, the pressure is only solved on the grid without the refinement and within the refinement; loops over the whole grid are avoided. The multi grid technique, on which the solver is based, will be explained shortly; many literature can be found that explains it in detail. Let us take the equation $A\mathbf{x} = \mathbf{b}$. The error in the approximation of $\mathbf{x}$ can be Fourier analyzed and will consist of high and low frequency components. The high frequency component is a local disturbance (noise) and this component of the error can easily be removed. More difficult are the low frequency components. Relative to the grid, these components are smooth and therefore well approximated on a coarser grid. The multi grid method takes care of these last components by the following procedure. First remove the high frequency components by means of smoothing. Call the true solution $\mathbf{x}$ and the approximation $\mathbf{y}$. Furthermore define the error $\mathbf{e} = \mathbf{x} - \mathbf{y}$

and the residue $\mathbf{r} = \mathbf{b} - A\mathbf{y}$. Then $A\mathbf{e} = A\mathbf{x} - A\mathbf{y} = \mathbf{b} - A\mathbf{y} = \mathbf{r}$. This is an equation for the error, its right hand side can be computed. Since the solution of this equation will be smooth, this equation can be solved on a coarser grid. After $\mathbf{e}$ has been solved on the coarser grid, $\mathbf{e}$ can be approximated on the whole grid. This approximation introduces new high frequency components in the error of $\mathbf{x}$, but after correcting $\mathbf{x}$ with $\mathbf{e}$ these can be removed again by smoothing.
In the case of local mesh refinement we want to eliminate the refinement nodes, such that the grid becomes regular. Outside the refinement the grid is not coarsened, so the error $\mathbf{e}$ will be representable without smoothing. As smoother Gauss-Seidel iteration is used. The following algorithm describes how the Poisson equation is solved.

- Iterate a few times with Gauss-Seidel on the refined part of the grid. If the coupling pressures are computed first, no further exception has to be made for the boundary of the refinement.
- Compute the residue on the whole grid.
- For each refined cell compute the sum of the nine accompanying residues. This sum is part of the right hand side of the equation on the regular grid.
- Solve the equation on the regular grid. Any method that can be used for solving Poisson equations on grids without refinement can be used for this equation.
- Approximate the solved error on the refined nodes with linear interpolation.
- Correct $\mathbf{y}$ with $\mathbf{e}$.
- Repeat the first step (smoothing).

If the error is still too large after these steps, the process can be repeated. However, in practice this appears to be unnecessary. The number of smoothing iterations could be adjusted each time step or fixed. In out experience five iterations suffice to get a large decrease of the residue. Solving the regular grid equation takes approximately the same time as solving the Poisson equation on the grid without refinement. Altogether, this is a very efficient and surveyable method. The only extra work for eight new unknown pressures consists of ten Gauss-Seidel iterations and computation of the residue. Furthermore, no large exceptions has to be made for the boundary and this algorithm is easily extended to two levels.

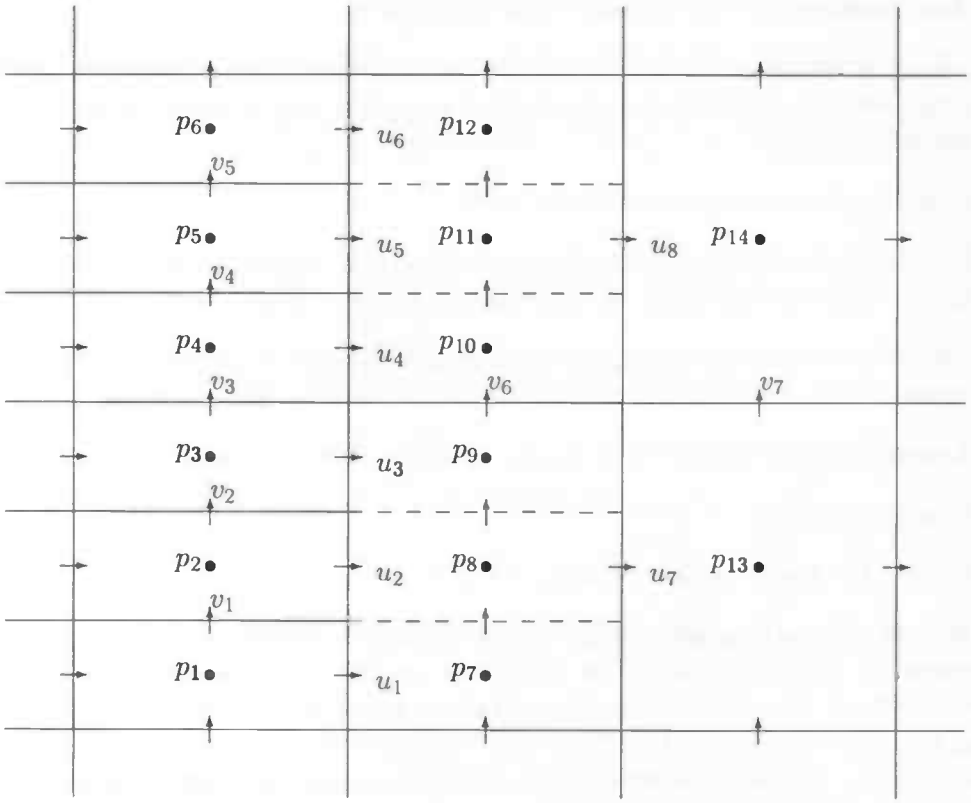

Figure 5.4: Grid used for deriving the Poisson matrix.

5.3 Convection at boundary of refinement

In this section we will discuss the transport by convection of fluid at the boundary of the refinement. As we have seen before, the convective term in the Navier Stokes equations should conserve energy after discretization. So we will try to use the freedom in the 'missing' velocities to globally preserve energy. We start with the x-direction, so the discretization of div(uu). In Figure 5.5 a part of the grid is drawn. The three u-cells of u_4, u_5 and u_6 are drawn in boldface.

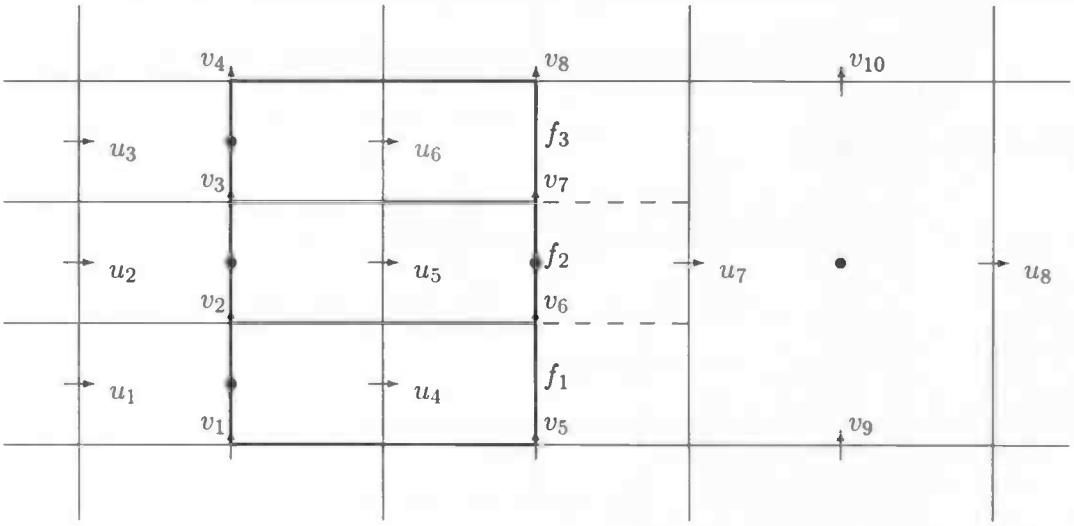

Figure 5.5: Discretization of convection in u-cells.

We will only pay attention at the right halves of these u-cells, since the other halve is regular. The variables v_6 and v_7 are virtual velocities and are still to be determined. Writing down the exact expressions for energy is quite a large job and therefore we will use the skew-symmetry rule that guarantees energy conservation. The three eastern boundaries of the u-cells of u_4, u_5 and u_6 are together the western boundary of u_4. Thus the sum of the momentum fluxes through these boundaries, denoted as f_1, f_2 and f_3, is the flux through the western boundary of the u-cell of u_4. Possible formulas for f_1, f_2 and f_3 with correct skew-symmetry properties are

$$\begin{aligned} f_1 &= \frac{u_4+u_7}{2}\frac{\bar{u}_4+\frac{1}{3}\bar{u}_7}{2}, \\ f_2 &= \frac{u_5+u_7}{2}\frac{\bar{u}_5+\frac{1}{3}\bar{u}_7}{2}, \\ f_3 &= \frac{u_6+u_7}{2}\frac{\bar{u}_6+\frac{1}{3}\bar{u}_7}{2}. \end{aligned}$$

Because then, for example, u_7 depends on u_4 with coefficient $-\frac{\bar{u}_4+\bar{u}_7}{4}$ and u_4 depends on u_7

with minus the same coefficient. The momentum fluxes of the u-cell of u_7 now becomes

$$\frac{u_7+u_8}{2}\frac{\bar{u}_7+\bar{u}_8}{2}+\frac{u_7+u_{7N}}{2}\frac{\bar{v}_8+\bar{v}_{10}}{2}-f_3-f_2-f_1-\frac{u_7+u_{7S}}{2}\frac{\bar{v}_5+\bar{v}_9}{2},$$

with u_{7N} and u_{7S} the northern and southern neighbour of u_7[1]. The central coefficient equals

$$\frac{\bar{u}_7+\bar{u}_8}{4}+\frac{\bar{v}_8+\bar{v}_{10}}{4}-\frac{\bar{u}_4+\frac{1}{3}\bar{u}_7}{4}-\frac{\bar{u}_5+\frac{1}{3}\bar{u}_7}{4}-\frac{\bar{u}_6+\frac{1}{3}\bar{u}_7}{4}-\frac{\bar{v}_5+\bar{v}_9}{4}=$$

$$\frac{\bar{u}_8+\bar{v}_{10}+\bar{v}_8-\bar{u}_6-\bar{u}_5-\bar{u}_4-\bar{v}_5-\bar{v}_9}{4}=0,$$

as one could already have seen in advance by looking at Figure 5.5. The balance of u_4 becomes

$$\frac{u_4+u_7}{2}\frac{\bar{u}_4+\frac{1}{3}\bar{u}_7}{2}+\frac{u_4+u_5}{2}\frac{\bar{v}_2+\bar{v}_6}{2}-\frac{u_4+u_1}{2}\frac{\bar{u}_4+\bar{u}_1}{2}-\frac{u_4+u_{4S}}{2}\frac{\bar{v}_1+\bar{v}_5}{2},$$

with central coefficient

$$\frac{\bar{u}_4+\frac{1}{3}\bar{u}_7}{4}+\frac{\bar{v}_2+\bar{v}_6}{4}-\frac{\bar{u}_4+\bar{u}_1}{4}-\frac{\bar{v}_1+\bar{v}_5}{4}=$$

$$\underbrace{\frac{\bar{u}_4+\bar{v}_2-\bar{u}_1-\bar{v}_1}{4}}_{=0}+\frac{\frac{1}{3}\bar{u}_7+\bar{v}_6-\bar{u}_4-\bar{v}_5}{4}.$$

We can choose v_6 such that $\bar{v}_6$ makes the expression zero:

$$\frac{1}{3}\bar{u}_7+\bar{v}_6-\bar{u}_4-\bar{v}_5=0.$$

By examining the central coefficient of u_6 we get an implicit definition of v_7:

$$\frac{1}{3}\bar{u}_7+\bar{v}_8-\bar{u}_6-\bar{v}_7=0.$$

The central coefficient of u_5 will become

$$\frac{\frac{1}{3}\bar{u}_7+\bar{v}_7-\bar{u}_5-\bar{v}_6}{4},$$

but this will also be zero, since $\bar{u}_7+\bar{v}_8-\bar{u}_6-\bar{u}_5-\bar{u}_4-\bar{v}_5=0$. The definitions of v_6 and v_7 can also be expressed in words: split the p-cell in the middle of Figure 5.5 into three pieces (along the dashed lines) and choose v_6 and v_7 such that each part is divergence free.
One could wonder whether other solutions for v_6 and v_7 exist with energy conservation. Indeed, this is the case if we assume the mass flux through the face with u_7 to have three different values. Looking at f_1, f_2 and f_3 one could observe that the coefficient of u_7 should contain the whole mass flux through the face with u_7 (divided by 4). So this mass flux can be split into three parts,

$$f_1=\frac{u_4+u_7}{2}\frac{\bar{u}_4+\lambda\bar{u}_7}{2},\quad f_2=\frac{u_5+u_7}{2}\frac{\bar{u}_5+\mu\bar{u}_7}{2},\quad f_3=\frac{u_6+u_7}{2}\frac{\bar{u}_6+(1-\lambda-\mu)\bar{u}_7}{2},$$

with λ and μ some parameters.

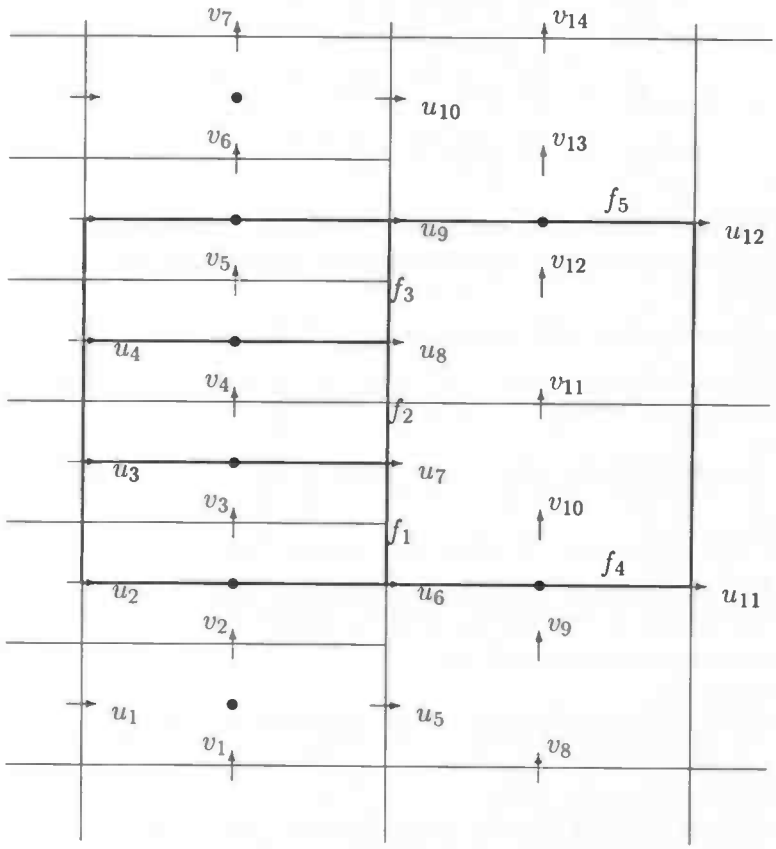

Figure 5.6: Discretization of convection in v-cells.

Next, we will look at the discretization of $\mathrm{div}(vu)$ in v-cells. See Figure 5.6 for the numbering. The discretization of the momentum fluxes of the v-cell of v_{11} is the hardest part. Normally, one would expect the central coefficient

$$\frac{1}{4}(\bar{u}_{11} + \bar{u}_{12} + \bar{v}_{14} - \bar{u}_{10} - \bar{u}_9 - \bar{u}_8 - \bar{u}_7 - \bar{u}_6 - \bar{u}_5 - \bar{v}_8).$$

But if

$$\begin{aligned} f_1 &= \frac{v_3 + v_{10}}{2}\frac{\bar{u}_6 + \bar{u}_7}{2}, \\ f_2 &= \frac{v_4 + v_{11}}{2}\frac{\bar{u}_7 + \bar{u}_8}{2}, \\ f_3 &= \frac{v_5 + v_{12}}{2}\frac{\bar{u}_8 + \bar{u}_9}{2}, \end{aligned}$$

then $\bar{u}_5$ and $\bar{u}_{10}$ will not occur in the central coefficient of v_{11}. One could think of averaging

[1]This notation will be used more frequently in the future and is not be defined explicitly anymore.

the mass flux, such that

$$\begin{aligned} f_1 &= \frac{v_3 + v_{10}}{2}\frac{\bar{u}_5 + \bar{u}_6 + \bar{u}_7}{3}, \\ f_2 &= \frac{v_4 + v_{11}}{2}\frac{\bar{u}_5 + \bar{u}_6 + \bar{u}_7 + \bar{u}_8 + \bar{u}_9 + \bar{u}_{10}}{6}, \\ f_3 &= \frac{v_5 + v_{12}}{2}\frac{\bar{u}_8 + \bar{u}_9 + \bar{u}_{10}}{3}. \end{aligned}$$

However, in this case the central coefficient of v_3, v_4 and v_5 will not vanish. Two ways to avoid this problem are presented, one that repairs the western flux of v_{11} and one that repairs f_4 and f_5.
The following discretization will preserve energy:

$$\frac{v_{11} + v_{11E}}{2}\frac{\bar{u}_{11} + \bar{u}_{12}}{2} + \frac{v_{11} + v_{14}}{2}\frac{\bar{v}_{11} + \bar{v}_{14}}{2} - \frac{v_{13} + v_6}{2}\frac{\bar{u}_9 + \bar{u}_{10}}{2} - \frac{v_{11} + v_4}{2}\frac{\bar{u}_7 + \bar{u}_8}{2} - \frac{v_9 + v_2}{2}\frac{\bar{u}_5 + \bar{u}_6}{2} - \frac{v_{11} + v_8}{2}\frac{\bar{v}_{11} + \bar{v}_8}{2},$$

with $v_{10} = v_8$ and $v_{12} = v_{14}$. It takes the eastern fluxes of the v-cell of v_2, v_4 and v_6, so not of v_3, v_4 and v_5 as one would expect. The choice of v_{10} and v_{12} then follows because of symmetry. If v_{11} has v_6 as neighbour, then v_6 should have v_{11} as neighbour. Otherwise, v_{11} does not see v_5, so v_{12} cannot equal v_{11}.
The other solution is

$$\frac{v_{11} + v_{11E}}{2}\frac{\bar{u}_{11} + \bar{u}_{12}}{2} + \frac{v_{11} + v_{14}}{2}m_N - \frac{v_{12} + v_5}{2}\frac{\bar{u}_8 + \bar{u}_9}{2} - \frac{v_{11} + v_4}{2}\frac{\bar{u}_7 + \bar{u}_8}{2} - \frac{v_{10} + v_3}{2}\frac{\bar{u}_6 + \bar{u}_7}{2} - \frac{v_{11} + v_8}{2}m_S,$$

with $v_{10} = v_{12} = v_{11}$ and the mass fluxes m_S and m_N such that the central coefficient equals zero:

$$\begin{aligned} m_S &= \frac{1}{2}\bar{u}_{11} + \bar{v}_{11} - \bar{u}_7 - \frac{1}{2}\bar{v}_6, \\ m_N &= -\frac{1}{2}\bar{u}_{12} + \frac{1}{2}\bar{u}_9 + \bar{u}_8 + \bar{v}_{11}. \end{aligned}$$

The v-cells of v_3, v_4 and v_5 will always have a zero central coefficient, since v_{10} and v_{12} do not occur on the diagonal of v_3, v_4 and v_5. Since the resulting coefficient matrix is skew-symmetric, the energy is conserved with one of the choices above.
Altogether we have found definitions for the missing velocities, in x- and y-direction, that guarantee energy conservation of the convective terms. Unfortunately, an example (Figure 5.7) shows that the discretization is not even first order, independent of the precise discretization used. The horizontal momentum flux at the left side of the grid equals

$$1 \cdot 1 \cdot \frac{1}{3} + 2 \cdot 2 \cdot \frac{1}{3} + 3 \cdot 3 \cdot \frac{1}{3} = 4\frac{2}{3}$$

and at the right side

$$2 \cdot 2 = 4.$$

So whatever discretization is used at the boundary, the situation of Figure 5.7 can never remain. The problem with this case is that the $u_i's$ vary too much at the boundary of the

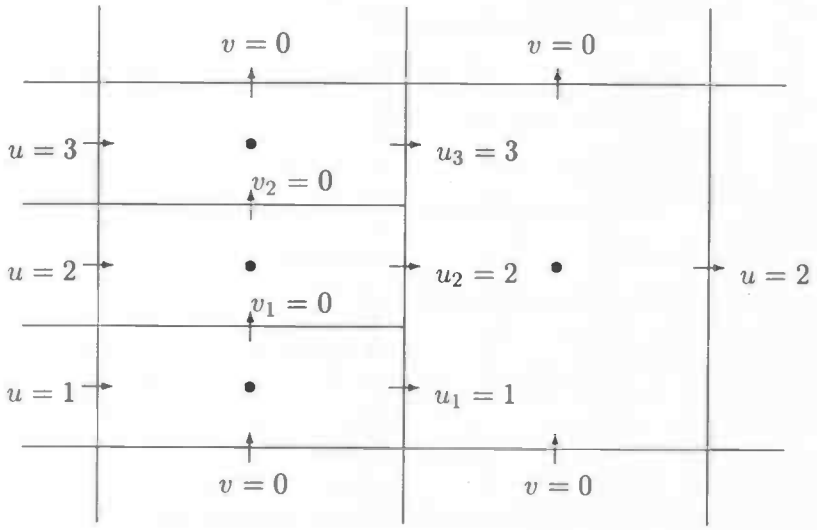

Figure 5.7: Test case energy preserving convection.

refinement. The situation that u is constant within one refined cell and u is globally linear could occur, see Figure 5.8.

We may expect that if the boundary is located in a region where the velocity and pressure is smooth, so do not vary much within a refined cell, the discretization will satisfy. To study this, some 2D simulations of the flow around a cube were done, see Figure 5.9. The coarse grid consisted of 100×100 cells, uniform in flow direction and in the other direction refinement near the channel boundaries. The Reynolds number was 200 based on the height of the obstacle. The dashed rectangle denotes the local refinement. Four positions of the eastern boundary of the refinement were used, denoted as A, B, C and D. Unfortunately, it appeared that vertical velocity at the eastern boundary was not smooth. Instead, the same vortices we have seen before are formed, see Figure 5.2. These vortices exist at the whole eastern boundary and vortices close to each other are rotating in the same direction. Therefore, the horizontal velocity components of these vortices cancel out and the horizontal velocity of the flow is not disturbed. One could wonder why only the eastern boundary suffers from this phenomenon. To start with the western boundary, it is noticed that convection and diffusion is not dominant. Only the pressure 'sees' an obstacle and sends this information upstream. The smooth transition at the western boundary is an indication that the pressure is handled well. At the northern and southern boundary convection is important, especially at the right part where the flow is turbulent. The difference is that the flow velocity along the boundary is large and the flow through the boundary small at the northern and southern boundary. This is opposite to the eastern boundary, where the flow velocity through the boundary is dominant. Apparently, under these circumstances vortices originate.

The magnitude of the wiggles were measured at a few moments in time when they were clearly visible. The wiggle was measured by taking three successive v_i's, with v_2 the last vertical velocity within the refinement and calculating $v_1 - 2v_2 + v_3$. It appeared that there was no clear relation between ℓ and the magnitude of the wiggles, see Figure 5.10. However, the

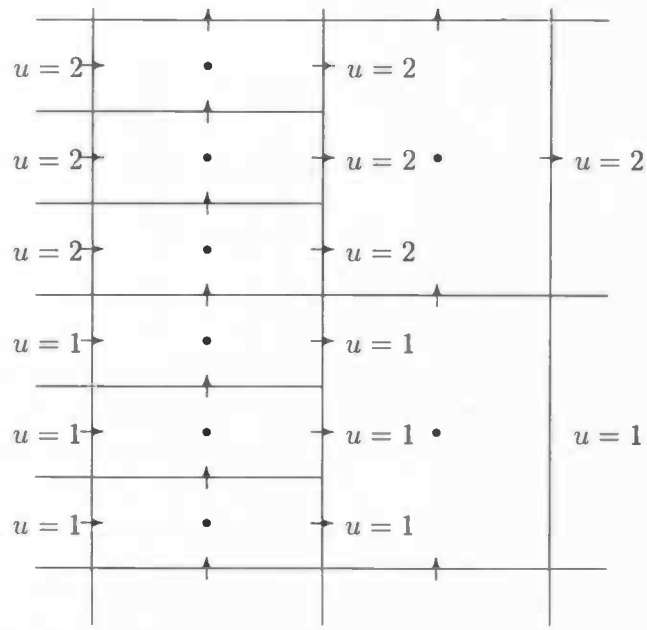

Figure 5.8: Constant horizontal velocity within refined cells.

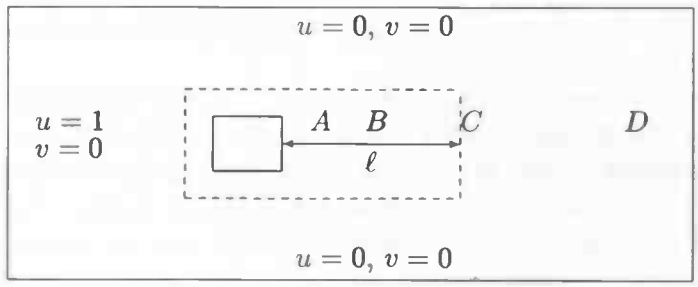

Figure 5.9: Channel flow around cube within refinement.

length of the area that is disturbed by the refinement boundary becomes larger for bigger ℓ and this makes the transition clearer visible for large ℓ.

Further research shows that the wiggles are caused by the jump in the horizontal mesh sizes. If a grid without local mesh refinement is discontinuous in the same way as it is with refinement (for example Figure 5.11), the wiggles also will occur. These wiggles are caused by an imperfection of the discretization of the $u\frac{\partial v}{\partial x}$ (and $v\frac{\partial u}{\partial y}$) term. If we look back at Figure 3.2 we may notice that the northern and southern boundary of the control volumes are not in the middle of the horizontal velocities. In spite of this we took the mean velocities $\frac{u_{ij}+u_{ij+1}}{2}$ and $\frac{u_{ij}+u_{ij-1}}{2}$ respectively. Dropping these weights $\frac{1}{2}$ will spoil energy conservation and cause even bigger problems therefore.

To study the consequences we will discretize the equation

$$\frac{\partial v}{\partial t} = c\frac{\partial v}{\partial x}$$

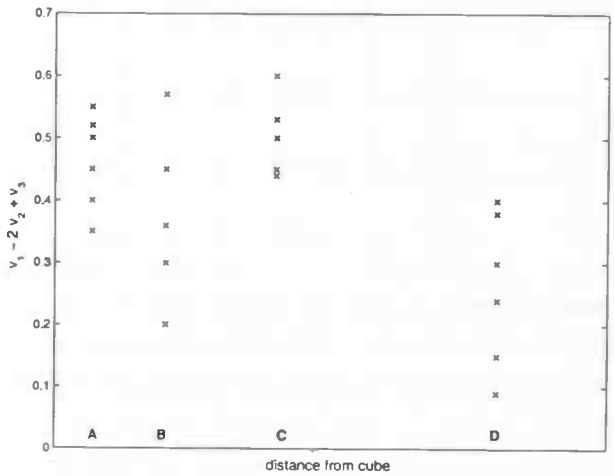

Figure 5.10: Magnitude of the wiggles for different positions of the eastern refinement boundary at various time steps.

with c a constant horizontal velocity. We used the grid drawn in Figure 5.11.

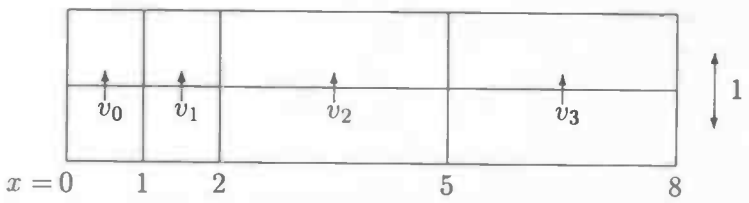

Figure 5.11: Grid with discontinuous grid sizes.

The finite volume discretization will become

$$\begin{aligned}
1\frac{\mathrm{d}v_0}{\mathrm{d}t} &= c\left(\frac{v_0+v_1}{2} - \frac{v_{0W}+v_0}{2}\right) &= \frac{c}{2}(v_1 - v_{0W}),\\
1\frac{\mathrm{d}v_1}{\mathrm{d}t} &= c\left(\frac{v_1+v_2}{2} - \frac{v_0+v_1}{2}\right) &= \frac{c}{2}(v_2 - v_0),\\
3\frac{\mathrm{d}v_2}{\mathrm{d}t} &= c\left(\frac{v_2+v_3}{2} - \frac{v_1+v_2}{2}\right) &= \frac{c}{2}(v_3 - v_1),\\
3\frac{\mathrm{d}v_3}{\mathrm{d}t} &= c\left(\frac{v_3+v_4}{2} - \frac{v_2+v_3}{2}\right) &= \frac{c}{2}(v_4 - v_2).
\end{aligned}$$

Next, we take v linear, for example $v = ax$, and substitute this:

$$1\frac{\mathrm{d}v_0}{\mathrm{d}t} = \tfrac{c}{2}a(\tfrac{3}{2}+\tfrac{1}{2}) = ac, \tag{5.4a}$$

$$1\frac{\mathrm{d}v_1}{\mathrm{d}t} = \tfrac{c}{2}a(\tfrac{7}{2}-\tfrac{1}{2}) = \frac{3}{2}ac, \tag{5.4b}$$

$$3\frac{\mathrm{d}v_2}{\mathrm{d}t} = \tfrac{c}{2}a(\tfrac{13}{2}-\tfrac{3}{2}) = \frac{5}{2}ac, \tag{5.4c}$$

$$3\frac{\mathrm{d}v_3}{\mathrm{d}t} = \tfrac{c}{2}a(\tfrac{19}{2}-\tfrac{7}{2}) = 3ac. \tag{5.4d}$$

All time derivatives should equal ac, but we notice that this does not hold for v_1 and v_2, so the velocities next to grid discontinuity. With this discretization v_1 will increase and v_2 will decrease. This is exactly the wiggle that often appears in the solution. The spatial discretized system is of the form

$$\Omega\frac{\mathrm{d}}{\mathrm{d}t}v = Cv.$$

The matrix C cannot easily be modified without spoiling its properties, but one could change the diagonal matrix Ω. Looking at Equations (5.4b) and (5.4c) one could suggest taking

$$\frac{3}{2}\frac{\mathrm{d}v_1}{\mathrm{d}t} = \frac{3}{2}ac,$$
$$\frac{5}{2}\frac{\mathrm{d}v_2}{\mathrm{d}t} = \frac{5}{2}ac.$$

This sum of the cell sizes is preserved ($2+2 = \frac{3}{2}+\frac{5}{2}$), but now the solution is exact for linear v. In general the new Ω_i can be defined as half the distance between both neighbouring v_i. What are the consequences of changing Ω_i? First take a look at its former definition. It is the discretization of

$$\int_\Omega v\,\mathrm{d}\Omega,$$

with Ω the v-cell of v_{ij}. This already defines the matrix Ω and therefore it is not very proper to redefine it. Indeed, if we look at the second dimension we notice that the $v\frac{\partial v}{\partial y}$ term is divided by the new volume too, but this is certainly wrong. The discretization of this term should not explicitly depend on distances in the x-direction. But the $\bar{v}$ contains the old width of the v-cell and this is divided by the new width and these distances will not cancel out anymore. This can only be justified by saying that the new matrix Ω is part of the time integration. The new values of Ω will make it more accurate. Steady state solutions are not modified since then the whole $\Omega\frac{\mathrm{d}}{\mathrm{d}t}v$ term equals zero. If the old volume is used for the y-direction and the new volume for the x-direction, the central coefficient will not vanish (the convection matrix has a non-zero diagonal) and energy is not conserved. The precise consequences of taking the 'wrong' area are not yet worked out, but the flow around the obstacle showed great improvement.

There possible is another solution that can only be used at the boundary of the refinement. The grid for this method is obtained by joining the last two columns of cells before the refinement boundary. The vertical velocities of the middle column (so v^N, v^C and v^S) are not moved to the middle of the new cells, see Figure 5.12 and (5.13).

The new grid has the advantage that the eastern as well as the western boundary of the v-cells are exactly in between the surrounding v_i's. A disadvantage is that the vertical boundaries

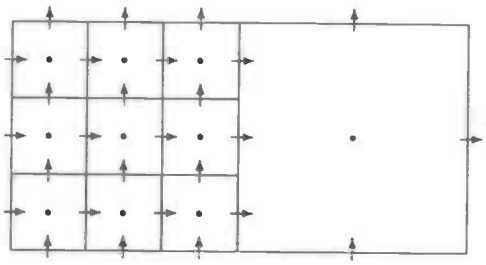

Figure 5.12: Normal transition from refined to normal grid.

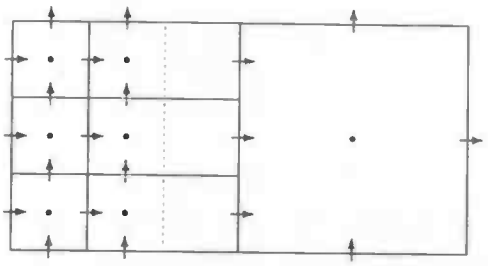

Figure 5.13: A more gradual transition from refined to normal grid.

of the u-cells are not centered anymore. The exact consequences of this choice are not yet known and further study is necessary. However, first results show great improvement.
Yet another solution is to modify the whole discretization, so the matrix C. One could think of taking a u-cell with all boundaries in the middle of two neighbouring u's. This approach will be explained in the next chapter.

Chapter 6

Future Work

Skew-symmetry of the convection matrix has appeared to be a very important property. One of its consequences is that the mean velocity at the boundary of a u-cell is the mean of the two neighbouring velocities. Physically, this can only be the right choice if the boundary of the u-cell is exactly in the middle of both velocities. Therefore will will propose a modification of the former discretization that has the boundaries of the u-cells in the middle. We will need a larger part of the grid to derive the discretization, see Figure 6.1.
Two different ways to discretize the convective term on the control volume of Figure 6.1 will be given. Both have in common that only the mass flux through the boundaries is modified, the mean velocity is left unchanged.

Averaged mass fluxes

We will first discuss the mass flux of the eastern boundary (formerly $\frac{u_{ij}+u_{i+1j}}{2}$). Again, the mass flux is constructed as the average of the fluxes through boundaries containing u_{ij} and u_{i+1j} (horizontal averaging). These fluxes are the half of $\bar{u}_{ij+1} + 2\bar{u}_{ij} + \bar{u}_{ij-1}$ and $\bar{u}_{i+1j+1} + 2\bar{u}_{i+1j} + \bar{u}_{i+1j-1}$ respectively (vertical averaging). So the mass flux becomes

$$\frac{1}{2}(\frac{1}{2}(\bar{u}_{ij+1} + 2\bar{u}_{ij} + \bar{u}_{ij-1}) + \frac{1}{2}(\bar{u}_{i+1j+1} + 2\bar{u}_{i+1j} + \bar{u}_{i+1j-1})).$$

For computing the mass flux through the northern boundary we notice that it is exactly in between u_{ij+1} and u_{ij}. Next, these fluxes are exactly in between boundaries containing vertical velocities. So this mass flux becomes

$$\frac{1}{2}(\frac{1}{2}(\bar{v}_{ij+1} + \bar{v}_{i+1j+1} + \bar{v}_{ij} + \bar{v}_{i+1j}) + \frac{1}{2}(\bar{v}_{ij} + \bar{v}_{i+1j} + \bar{v}_{ij-1} + \bar{v}_{i+1j-1})).$$

The western and southern boundary can be computed analogously, yielding

$$\frac{1}{2}(\frac{1}{2}(\bar{u}_{i-1j+1} + 2\bar{u}_{i-1j} + \bar{u}_{i-1j-1}) + \frac{1}{2}(\bar{u}_{ij+1} + 2\bar{u}_{ij} + \bar{u}_{ij-1}))$$

and

$$\frac{1}{2}(\frac{1}{2}(\bar{v}_{ij} + \bar{v}_{i+1j} + \bar{v}_{ij-1} + \bar{v}_{i+1j-1}) + \frac{1}{2}(\bar{v}_{ij-1} + \bar{v}_{i+1j-1} + \bar{v}_{ij-2} + \bar{v}_{i+1j-2}))$$

respectively.
Obviously, the skew-symmetry of the convection matrix is preserved with the new mass fluxes, if the diagonal equals zero. This property has to be verified, but rearranging shows that the

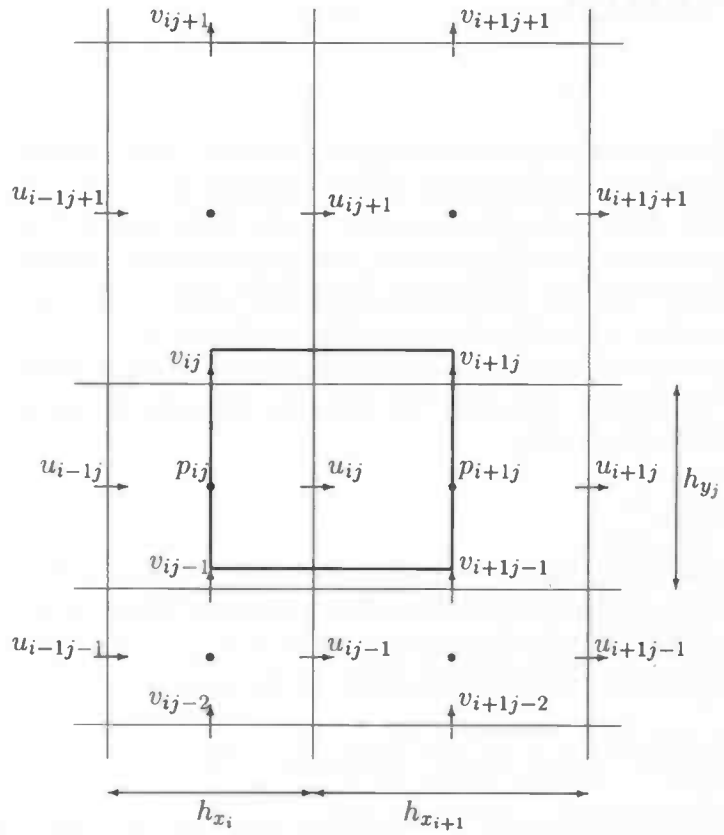

Figure 6.1: Control volume for discretization in x-direction

central coefficient contains the mass fluxes of cells (i,j) and $(i+1,j)$ with a factor $\frac{1}{2}$ and the mass fluxes of cells $(i,j+1)$, $(i+1,j+1)$, $(i,j-1)$ and $(i+1,j-1)$ with a factor $\frac{1}{4}$ and equals zero therefore.

Weighted mass fluxes

Another possible discretization is obtained if the mass fluxes of the original discretization are corrected for 'missing' or 'extra' parts. We will introduce two dimensionless parameters λ and μ:

$$\lambda h_{y_j} = \underbrace{\frac{1}{4}(y_j + 2y_{j-1} + y_{j-2})}_{\substack{y\text{-co-ordinate of} \\ \text{southern boundary}}} - y_j, \qquad \mu h_{y_{j+1}} = \underbrace{\frac{1}{4}(y_{j+1} + 2y_j + y_{j-1})}_{\substack{y\text{-co-ordinate of} \\ \text{northern boundary}}} - y_{j+1}.$$

The mass flux through the eastern boundary is now given by

$$(1-\lambda)\frac{\bar{u}_{ij} + \bar{u}_{i+1j}}{2} + \mu\frac{\bar{u}_{ij+1} + \bar{u}_{i+1j+1}}{2}.$$

The mass flux through the northern boundary is the linear interpolation of $\frac{\bar{v}_{ij}+\bar{v}_{i+1j}}{2}$ and $\frac{\bar{v}_{ij+1}+\bar{v}_{i+1j+1}}{2}$:

$$\mu\frac{\bar{v}_{ij+1} + \bar{v}_{i+1j+1}}{2} + (1-\mu)\frac{\bar{v}_{ij} + \bar{v}_{i+1j}}{2}.$$

The western boundary is analogue to the eastern boundary, yielding

$$(1-\lambda)\frac{\bar{u}_{ij} + \bar{u}_{i-1j}}{2} + \mu\frac{\bar{u}_{ij+1} + \bar{u}_{i-1j+1}}{2}$$

and for the southern boundary

$$\lambda\frac{\bar{v}_{ij} + \bar{v}_{i+1j}}{2} + (1-\lambda)\frac{\bar{v}_{ij-1} + \bar{v}_{i+1j-1}}{2}.$$

Again, we should examine the central coefficient. As we had before, the central coefficient is a combination of the mass flows of the concerning p-cells: $\frac{\mu}{2}$ of cells $(i,j+1)$ and $(i+1,j+1)$ and $\frac{1-\lambda}{2}$ of cells (i,j) and $(i+1,j)$. The mass flows of cells $(i,j-1)$ and $(i+1,j-1)$ do not occur, but this is determined by the particular way of stretching used in the example.

Discussion

Both discretizations have the property that horizontal momentum that is linear in the y-direction and transported by a uniform vertical velocity field is an exact solution of the discretized equations. If both u and v are linear, the discretization will not be exact on non-uniform grids, due to the fact that the velocities are not in the middle of their cell.
The discretization with the averaged mass fluxes has the property that it 'average very much', even on a uniform grid. Therefore, we may expect less accurate results on uniform or smoothly stretched grids. Another disadvantage is that the stencil is larger than it was. Therefore exceptions has to be made at boundaries.
The second discretization has the pleasant property that it reduces to the original discretization at uniform grids. On non-uniform grids the stencil will also be larger, but now no exceptions have to be made near boundaries.
Both methods show great improvement, but further research is necessary to study the differences with the former discretization.

Chapter 7

Conclusions

In this thesis we derived a discretization at the boundary of local mesh refinement that conserves mass, momentum as well as kinetic energy.
The mass equation appears to be correctly discretized and does not cause any trouble. The accompanying Poisson equation for the pressure is efficiently solved. Therefore, the time gained by saving grid cells is not lost due to the irregularity of the grid making local grid refinement a powerful tool.
Expressions for the 'missing' velocities of the discrete momentum equations are given, such that momentum and energy are conserved. In combination with one dimensional refinement this functions well. With two dimensional refinement the discontinuity of the grid cells causes wiggles in the solution. In fact, one cannot blame the local mesh refinement, a regular grid with a jump in the cell sizes would suffer from the same problem. To solve these problems a few possible solutions that change the discretization locally or globally are given. These new discretizations show great improvement, but are still not perfect yet. Further investigation has to be done in this area.